AMERICAN SOCIETY FOR MICROBIOLOGY | mBio®

RESEARCH ARTICLE

# Mucosal BCG Vaccination Induces Protective Lung-Resident Memory T Cell Populations against Tuberculosis

**Carolina Perdomo,[a] Ulrike Zedler,[a] Anja A. Kühl,[b] Laura Lozza,[a] Philippe Saikali,[a] Leif E. Sander,[c] Alexis Vogelzang,[a] Stefan H. E. Kaufmann,[a] Andreas Kupz[a,d]**

Department of Immunology, Max Planck Institute for Infection Biology, Berlin, Germany[a]; Department of Medicine, Charité University Hospital, Berlin, Germany[b]; Department of Infectious Diseases and Pulmonary Medicine, Charité University Hospital, Berlin, Germany[c]; Centre for Biosecurity and Tropical Infectious Diseases, Australian Institute of Tropical Health and Medicine, James Cook University, Cairns, Queensland, Australia[d]

A.V., S.H.E.K., and A.K. contributed equally to this work.

**ABSTRACT** ***Mycobacterium bovis*** **Bacille Calmette-Guérin (BCG) is the only licensed vaccine against tuberculosis (TB), yet its moderate efficacy against pulmonary TB calls for improved vaccination strategies. Mucosal BCG vaccination generates superior protection against TB in animal models; however, the mechanisms of protection remain elusive. Tissue-resident memory T ($T_{RM}$) cells have been implicated in protective immune responses against viral infections, but the role of $T_{RM}$ cells following mycobacterial infection is unknown. Using a mouse model of TB, we compared protection and lung cellular infiltrates of parenteral and mucosal BCG vaccination. Adoptive transfer and gene expression analyses of lung airway cells were performed to determine the protective capacities and phenotypes of different memory T cell subsets. In comparison to subcutaneous vaccination, intratracheal and intranasal BCG vaccination generated T effector memory and $T_{RM}$ cells in the lung, as defined by surface marker phenotype. Adoptive mucosal transfer of these airway-resident memory T cells into naive mice mediated protection against TB. Whereas airway-resident memory $CD4^+$ T cells displayed a mixture of effector and regulatory phenotype, airway-resident memory $CD8^+$ T cells displayed prototypical $T_{RM}$ features. Our data demonstrate a key role for mucosal vaccination-induced airway-resident T cells in the host defense against pulmonary TB. These results have direct implications for the design of refined vaccination strategies.**

**IMPORTANCE** **BCG remains the only licensed vaccine against TB. Parenterally administered BCG has variable efficacy against pulmonary TB, and thus, improved prevention strategies and a more refined understanding of correlates of vaccine protection are required. Induction of memory T cells has been shown to be essential for protective TB vaccines. Mimicking the natural infection route by mucosal vaccination has been known to generate superior protection against TB in animal models; however, the mechanisms of protection have remained elusive. Here we performed an in-depth analysis to dissect the immunological mechanisms associated with superior mucosal protection in the mouse model of TB. We found that mucosal, and not subcutaneous, BCG vaccination generates lung-resident memory T cell populations that confer protection against pulmonary TB. We establish a comprehensive phenotypic characterization of these populations, providing a framework for future vaccine development.**

**Received** 12 September 2016 **Accepted** 26 October 2016 **Published** 22 November 2016

**Citation** Perdomo C, Zedler U, Kühl AA, Lozza L, Saikali P, Sander LE, Vogelzang A, Kaufmann SHE, Kupz A. 2016. Mucosal BCG vaccination induces protective lung-resident memory T cell populations against tuberculosis. mBio 7(6):e01686-16. doi:10.1128/mBio.01686-16.

**Editor** Rino Rappuoli, GSK Vaccines



Address correspondence to Stefan H. E. Kaufmann, kaufmann@mpiib-berlin.mpg.de.

Since its introduction almost a century ago (1), live attenuated *Mycobacterium bovis* Bacille Calmette-Guérin (BCG) remains the only licensed vaccine against tuberculosis (TB) caused by the intracellular pathogen *Mycobacterium tuberculosis*. Although originally applied orally, today BCG is administered intradermally in early childhood and effectively prevents extrapulmonary TB, mainly disseminated miliary and meningeal forms in children (2). However, BCG fails to confer sufficient protection against the most common form of the disease, pulmonary TB. Thus, TB continues to cause significant global morbidity and mortality (3). The development and implementation of new and more efficient vaccines is mandatory if TB morbidity and mortality are to be reduced by 90 and 95%, respectively, to achieve the 2035 goal of the Stop TB Partnership (4, 5).

Induction of memory T cells has been shown to be essential for protective TB vaccines (6). In mice, protection against an *M. tuberculosis* challenge following subcutaneous (s.c.) BCG vaccination is dependent on T helper type 1 (Th1) $CD4^+$ T cell responses (7, 8). However, one of the shortcomings of s.c. BCG administration is the overall weak memory lymphocyte generation, which in addition lacks the mucosal-homing chemokine receptors that allow migration to the lung (9). Hence, mucosal vaccination has been suggested as a mimic of natural infection in order to improve local immunity at the site of infection (10–12). Comprehensive analyses of local immunity and correlates of protection in both the lung airways and the parenchyma are essential for the rational design of mucosal TB vaccination strategies using BCG (13, 14). Airway luminal T cells have been found to be critical for protec-

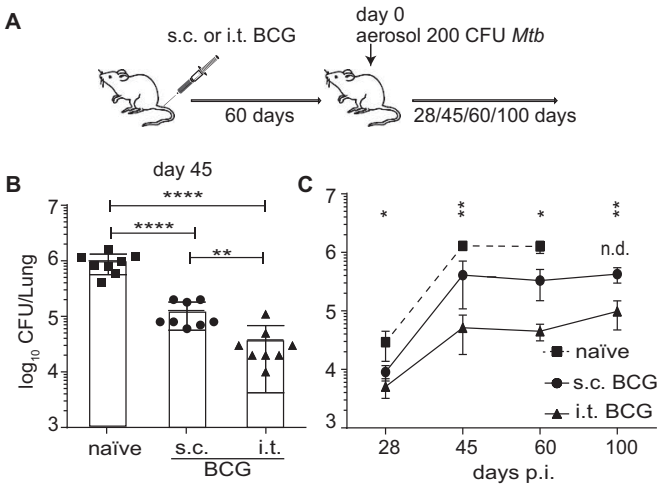


**FIG 1** Mucosal BCG vaccination confers improved protection against *M. tuberculosis* infection. (A) B6 mice were BCG vaccinated either i.t. or s.c. Sixty days later, vaccinated and control groups were aerosol infected with a low dose of virulent *M. tuberculosis* and the CFU counts in their lungs were determined at the time points indicated. (B, C) Individual $\log_{10}$ CFU counts per lung (48) at day 45 p.i. (B) and mean $\log_{10}$ CFU counts per lung from two pooled independent experiments ± the standard error of the mean at the time points indicated ($n = 8$ mice per group) (C). The statistical significance of differences between the s.c. and i.t. BCG vaccination routes is shown. ****, $P \leq 0.0001$; **, $P \leq 0.01$; *, $P \leq 0.05$; n.d., not done (analysis of variance with Tukey's posttest for significance).

tion against TB (15). However, in-depth characterization of infiltrating antigen-specific immune cell populations, in particular localization and function of tissue resident memory T ($T_{RM}$) cell subsets generated by mucosal vaccination, is still lacking.

Until recently, memory T cells were subdivided into two main subsets (16). First, T cells expressing high levels of CD62L, termed central memory T ($T_{CM}$) cells, migrate to lymphoid organs in response to L-selectin ligands, and second, low levels of CD62L mark T effector memory T ($T_{EM}$) cells, which recirculate between blood and peripheral tissues, where they are thought to survey the initial portals of infection (17). More recently, a third subset of memory T cells, $T_{RM}$ cells, which permanently resides in nonlymphoid tissues, has been mostly described (18) as $CD69^+$ $CD103^+$. Because of their strategic location and rapid recall response, $T_{RM}$ cells represent preferred cellular targets for efficacious vaccination. Whether mucosal BCG vaccination generates protective $T_{RM}$ cells in the lung remains to be explored. Our study investigated the hypothesis that an accumulation of *Mycobacterium*-specific lung-resident T cells, some of them expressing the $T_{RM}$ phenotype, underpins the improved protection against TB seen following the mucosal administration of BCG.

## RESULTS

**Mucosal BCG vaccination confers superior protection against *M. tuberculosis* infection.** To investigate the role of lung-resident T cells in immune protection against TB following BCG vaccination, we compared local (mucosal) BCG vaccination via the intratracheal (i.t.) route to parenteral vaccination by s.c. administration of BCG. Sixty days after vaccination, mice were challenged aerogenically with *M. tuberculosis* and the bacterial loads in their lungs were determined at various time points postinfection (p.i.) (Fig. 1A). Confirming recent studies (19, 20), we found that mucosal BCG vaccination confers better protection against *M. tuberculosis* infection than parenteral s.c. BCG vaccination for at least 100 days (Fig. 1B and C).

**Mucosal BCG vaccination generates a transient influx of *Mycobacterium*-specific $CD4^+$ and $CD8^+$ T cells into the lung parenchyma.** To identify possible mechanisms of improved protection following i.t. BCG vaccination, we performed a histological analysis of lung-infiltrating immune cells. Sixty days after mucosal vaccination (immediately prior to infection), unperfused lungs displayed greater cell infiltration and higher histological scores than those of naive and s.c. BCG-vaccinated mice (Fig. 2A and C, top). A large proportion of lung-infiltrating cells were $CD3^+$ T cells, many of which were $CD4^+$ (Fig. 2A and C, bottom). In contrast, 45 days after *M. tuberculosis* infection, there were no significant differences in the total number of T cells among the groups despite the lower histological scores of BCG-vaccinated animals (Fig. 2B and C).

To determine whether lung-infiltrating T cells were located in the lung parenchyma or the lung airways, we first removed the bronchoalveolar lavage fluid (BALF) and performed flow cytometry of the lung parenchyma tissue. Mucosal BCG vaccination induced higher numbers of $CD4^+$ and $CD8^+$ T cells in the lung parenchyma between days 22 and 45 following BCG vaccination (Fig. 2D, top). Intriguingly, this increase proved to be transient, as by day 60, the day of an *M. tuberculosis* challenge, there were no significant differences in the total lung parenchyma-infiltrating T cell numbers between the vaccination routes (Fig. 2D, top). At that time point, approximately 100 BCG CFU were detected in the lung (see Fig. S1A in the supplemental material). The majority of lung-parenchyma-infiltrating T cells displayed a memory phenotype, and a proportion stained positive for major histocompatibility complex (MHC) peptide tetramers derived from dominant mycobacterial antigens, namely, Ag85B-specific $CD4^+$ (Ag85B: H-2I-$A^b$) and TB10.4-specific $CD8^+$ (TB10.4:H-2$K^b$) T cell subpopulations (Fig. 2D, bottom; see Fig. S1B). However, apart from a small number of persisting TB10.4$^+$-specific $CD8^+$ T cells, the overall numbers of antigen-specific $CD4^+$ and $CD8^+$ T cells were comparable between the i.t. and s.c. BCG-vaccinated groups directly before an *M. tuberculosis* challenge (Fig. 2D, bottom) (21). Furthermore, no significant differences in the numbers of lung alveolar macrophages (AMs) ($CD11c^{hi}$ $CD11b^{lo}$ $F4/80^+$), dendritic cells (DCs) ($CD11c^{hi}$ $CD11b^{lo}$ $F4/80^{lo}$ MHC class $II^{hi}$) or neutrophils ($CD11b^{hi}$ $Ly6G^{hi}$) were observed over time between the two routes of vaccination, which suggests that changes in the myeloid compartment did not underlie increased protection (see Fig. S1C). Collectively, these results suggest that mucosal BCG vaccination drives a transient increase in *Mycobacterium*-specific $CD4^+$ and $CD8^+$ T cell populations in the lung parenchyma that recedes before a challenge.

**I.t. BCG vaccination generates T cells seeding the lung airways.** To further determine the contribution of airway-resident immune cells to improved vaccine-mediated protection, we collected BALF and performed a comprehensive analysis of airway-infiltrating cells in response to BCG vaccination and *M. tuberculosis* challenge. Analysis of the proportional changes in lumen-resident cell types revealed a cellular composition skewed toward resident lymphocytes following mucosal vaccination (Fig. 3A; see Fig. S2A). Although the total cell numbers in the BALF were comparable (see Fig. S2B), increased and decreased frequencies in airway cell populations were also reflected in the

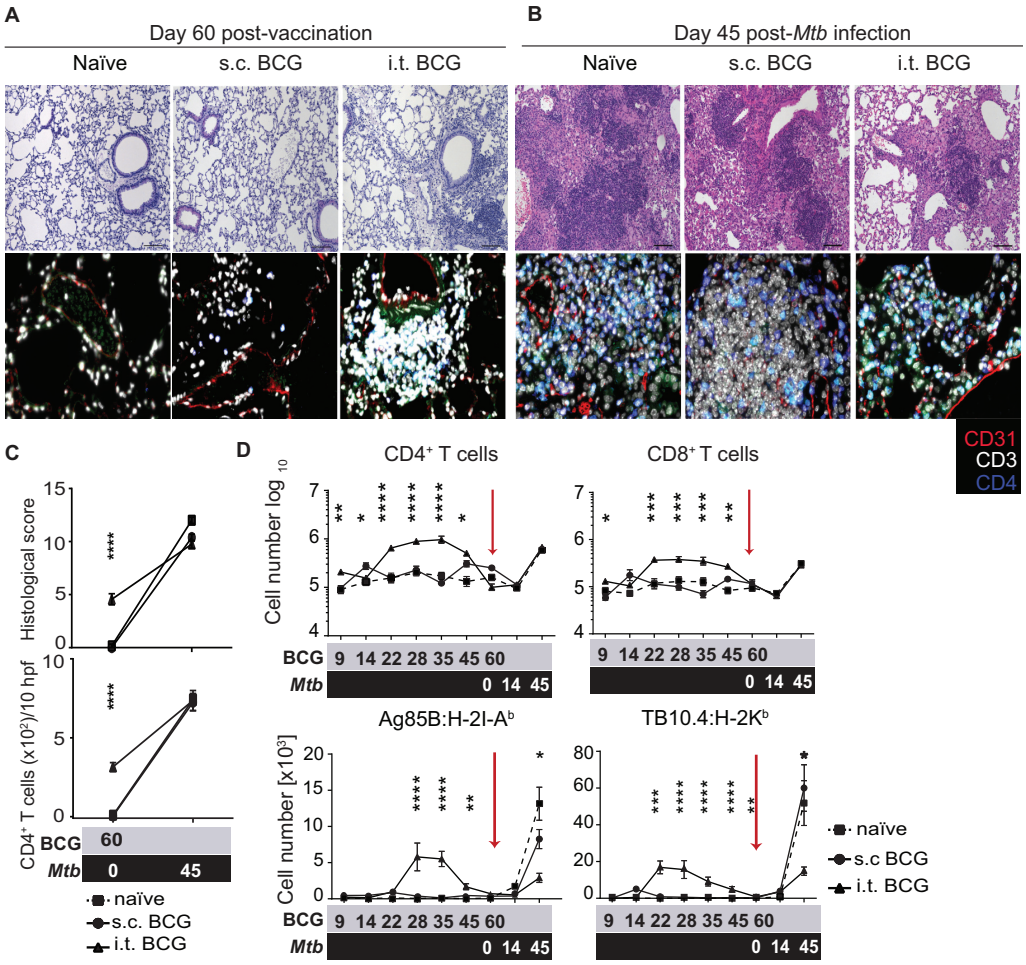


**FIG 2** I.t. BCG vaccination causes transient influx of T cells into the lung parenchyma. Histological staining of lung sections from control and i.t. or s.c. BCG-vaccinated mice 60 days after BCG immunization (A) and on day 45 after *M. tuberculosis* infection (B). Lung sections were stained with H&E (top) and IF (bottom) for CD31 (red), CD3 (white), and CD4 (blue). (C) Histological scores (top) and numbers of $CD4^+$ T cells per 10 high-power fields (hpf) (bottom) at designated time points after BCG vaccination (gray) and an *M. tuberculosis* challenge (black). Scale bar, 100 $\mu$m. Flow cytometric quantification of lung parenchyma (D) $TCR\beta^+$ $CD4^+$ and $CD8^+$ T cells (top) and antigen-specific Ag85B:H-2I-$A^b$ $CD4^+$ and TB10.4:H-2$K^b$ $CD8^+$ T cells (bottom) at designated time points after BCG vaccination (gray) and an *M. tuberculosis* challenge (black). Results are presented as mean values ± the standard error of the mean from two pooled independent experiments ($n = 8$ to 10 mice per group). The statistical significance of differences between s.c. and i.t. BCG immunizations is shown. ****, $P \leq 0.0001$; ***, $P \leq 0.001$; **, $P \leq 0.01$; *, $P \leq 0.05$. (C, D) Analysis of variance with Tukey's posttest for significance.

total cell numbers (see Fig. S2C). In contrast to the kinetics of local parenchymal T cell populations, we identified increased frequencies and numbers of airway luminal T cells after i.t. BCG vaccination that persisted until the challenge (Fig. 3B). Influx of T cells into the lung airways was detected at later experimental time points than parenchymal infiltration and started around day 24 after vaccination. Most strikingly, i.t. BCG vaccination led to a profound change in the composition of lung-residing immune cells that was characterized by a numerical and proportional increase in T cells (Fig. 3B; see Fig. S2A), many of which were specific for mycobacterial antigens by tetramer staining (Fig. 3C; see Fig. S3). Additionally, CXCR3, a chemokine receptor required for migration of T cells into the lung airways and parenchyma (22), was highly expressed on antigen-specific T cells after i.t. BCG vaccination (Fig. 3D), indicating recent targeted migration to the lung airways.

**$T_{EM}$ and $T_{RM}$ cells infiltrate the lung airways after i.t. BCG vaccination.** Because of the striking increase in the number of luminal T cells following i.t. vaccination, we interrogated whether airway-infiltrating T cells following i.t. BCG administration phenotypically resembled $T_{EM}$ ($CD44^{hi}$ $CD62L^{lo}$ $CD69^{lo}$) and $T_{RM}$ ($CD44^{hi}$ $CD62L^{lo}$ $CD103^+$ $CD69^+$) cells. Particularly the $T_{RM}$ population has been shown to confer protection against viral and bacterial pulmonary infections (23, 24). We found that, indeed, i.t. BCG vaccination recruited significantly higher frequencies and absolute numbers of $CD4^+$ and $CD8^+$ $T_{RM}$ and $T_{EM}$ cells to the airways than s.c. BCG vaccination (Fig. 4A and B). Similarly, characterization of parenchymal T cells revealed higher numbers of $CD4^+$ and $CD8^+$ $T_{EM}$ and $T_{RM}$ cells in i.t. BCG-vaccinated mice (Fig. 4C). Collectively, our results demonstrate that i.t. BCG vaccination induces $CD4^+$ and $CD8^+$ $T_{EM}$ and $T_{RM}$ cell recruitment to the lung airway spaces and the lung parenchyma.

**Phenotypic characterization of airway-infiltrating T cells generated by i.t. BCG vaccination.** $T_{RM}$ cells vary in phenotype and function, depending on the tissue they reside in (25–27). The phenotype of $T_{RM}$ cells in lung airways following mucosal BCG vaccination has not been characterized. Hence, we performed

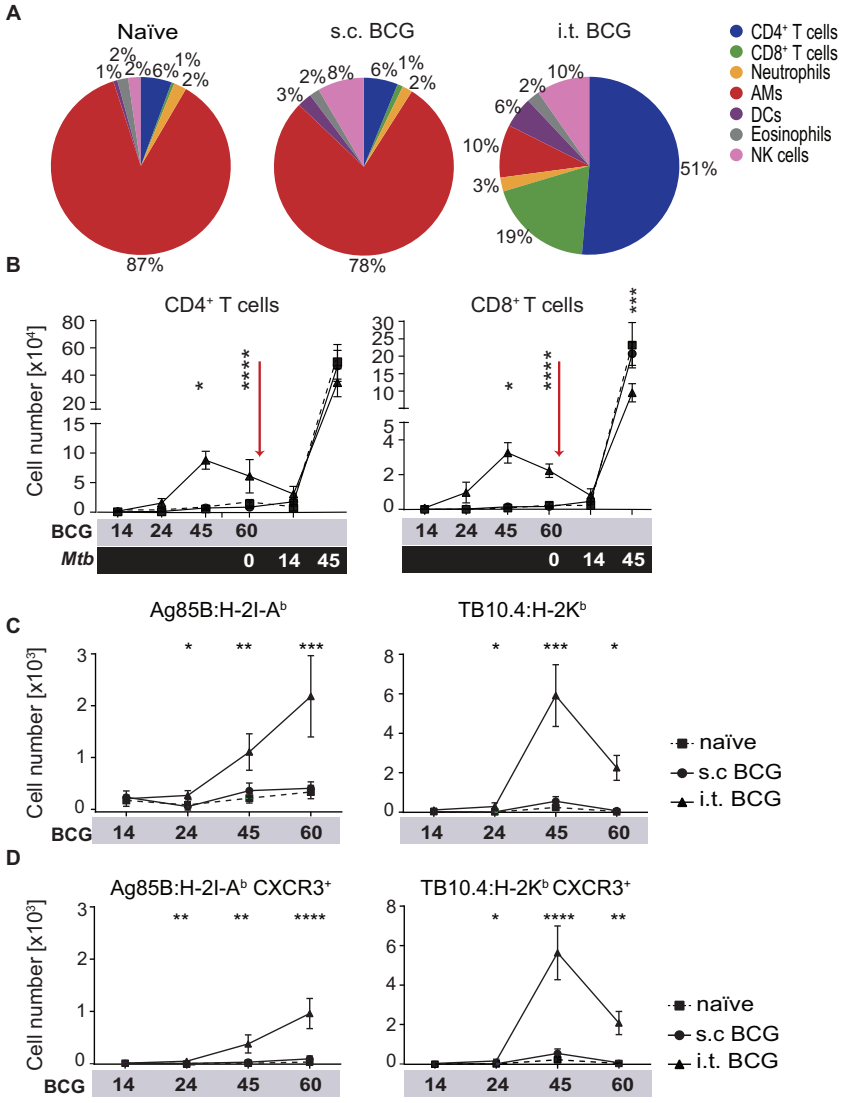


**FIG 3** I.t. BCG vaccination generates T cells seeding the lung airways. (A) Pie charts illustrating the composition of BALF cell populations as proportions of the total leukocytes from naive mice and mice at 60 days after BCG vaccination. (B) Flow cytometric quantification of total TCR$\beta^+$ CD4$^+$ and CD8$^+$ T cells in BALF at the time points indicated after BCG vaccination (gray) and an *M. tuberculosis* challenge (black). (C, D) Quantification of total BALF TCR$\beta^+$ Ag85B:H-2I-A$^b$ CD4$^+$ and TB10.4:H-2K$^b$ CD8$^+$ T cells (C) and TCR$\beta^+$ Ag85B:H-2I-A$^b$ CD4$^+$ and TB10.4:H-2K$^b$ CD8$^+$ T cells expressing CXCR3 (D) at designated time points after BCG vaccination. Results are presented as pooled mean data ± the standard error of the mean (B to D) or representative images (A) from two pooled independent experiments ($n = 6$ to 8 mice per group). The statistical significance of differences between s.c. and i.t. BCG vaccinations is shown. ****, $P \leq 0.0001$; ***, $P \leq 0.001$; **, $P \leq 0.01$; *, $P \leq 0.05$. (B to D) Analysis of variance with Tukey's posttest for significance.

transcriptional gene expression profiling of sorted BALF CD4$^+$ and CD8$^+$ $T_{EM}$ and $T_{RM}$ cell subpopulations induced by i.t. BCG vaccination with a Fluidigm Dynamic Array. The purity of the different sorted cell populations was routinely assessed at 86 to 99% (see Fig. S4). Increased transcription levels of typical markers associated with tissue residency of CD4$^+$ and CD8$^+$ $T_{RM}$ such as *Itgae* (CD103) and *Itga1* (VLA-1) were confirmed (Fig. 5A and B). CD4$^+$ $T_{RM}$ cells displayed a regulatory profile, with high *Foxp3* and *Il10* mRNA expression (Fig. 5A and B). Additionally, CD4$^+$ $T_{RM}$ cells expressed T-bet, as well as Foxp3, at the protein level (Fig. 5C). Importantly, each marker was expressed by distinct subpopulations, suggesting a heterogeneous population comprising effector and regulatory T cells (28). Therefore, we concluded that CD4$^+$ $T_{RM}$ cells, defined here as CD4$^+$ CD103$^+$ CD69$^+$ cells, comprise a mixture of regulatory and effector T cells rather than solely belonging to the $T_{RM}$ subset. On the other hand, CD8$^+$ $T_{RM}$ cells expressed significantly higher levels of gamma interferon (IFN-γ) (*Ifng*), tumor necrosis factor alpha (TNF-α) (*Tnfa*), and *Cxcr6* (Fig. 5B) (29) and statistically insignificantly higher levels of perforin (*Prf1*) and granzyme B (*Gzmb*) than their CD8$^+$ $T_{EM}$ counterparts (Fig. 5A).

To further characterize the phenotypes of $T_{EM}$ and $T_{RM}$ cells infiltrating the airways after i.t. BCG vaccination, we also assessed interleukin-2 (IL-2) receptor alpha chain (CD25), IFN-γ, and CXCR3 protein expression levels. I.t. BCG vaccination generated CD25- and CXCR3-expressing, IFN-γ-producing CD8$^+$ $T_{RM}$ cells, as well as CXCR3$^+$-expressing, IFN-γ-producing CD4$^+$ airway-resident T cell subpopulations (Fig. 5D). Collectively,

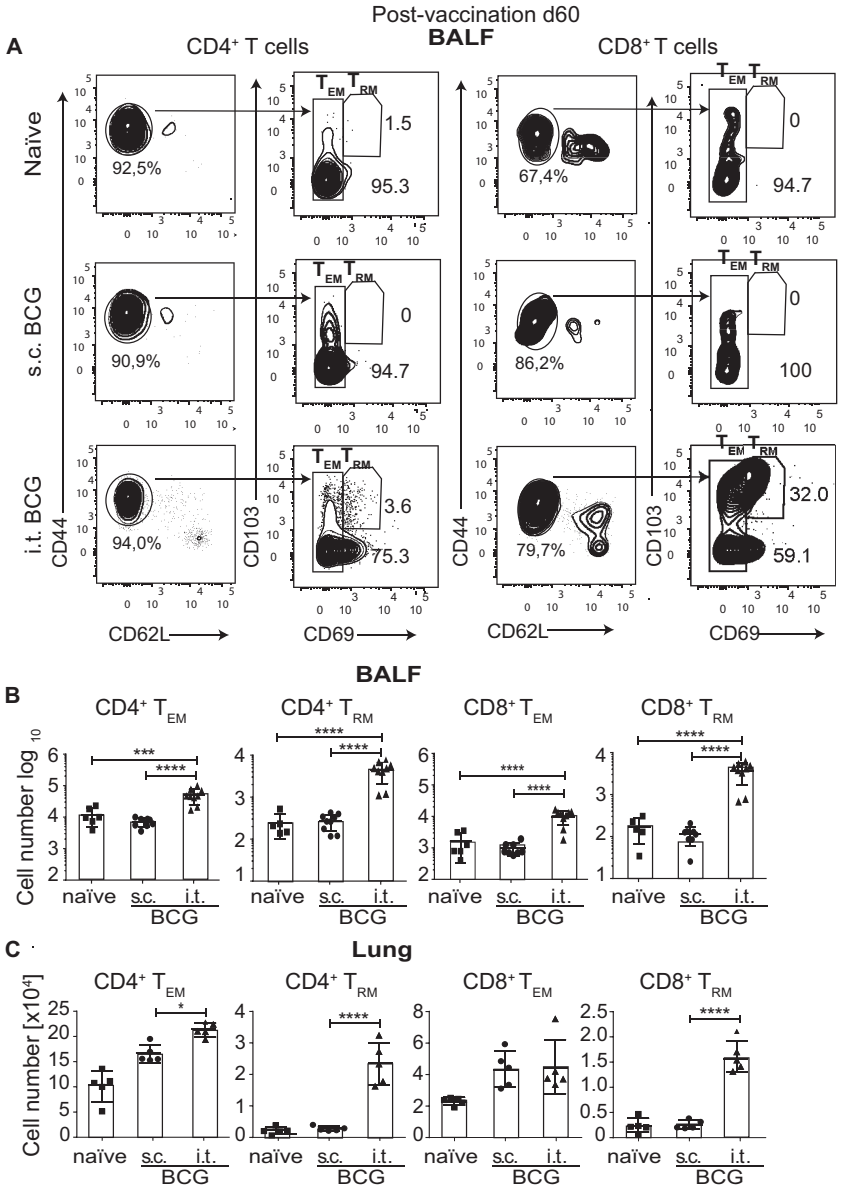


**FIG 4** $T_{EM}$ and $T_{RM}$ cells infiltrate the lung airways after i.t. BCG vaccination. (A) Representative flow cytometry gating strategy for $T_{EM}$ and $T_{RM}$ cells among $CD4^+$ and $CD8^+$ T cells at day 60 after BCG immunization in BALF pregated on TCR$\beta^+$ $CD4^+$ or TCR$\beta^+$ $CD8^+$ T cells. (B, C) Quantification of total $CD4^+$ $T_{EM}$, $CD4^+$ $T_{RM}$, $CD8^+$ $T_{EM}$, and $CD8^+$ $T_{RM}$ cells by flow cytometry 60 days after BCG vaccination in BALF (B) and lung parenchyma (C). Results are presented as pooled mean data ± the standard error of the mean plus individual data points (B, C) or representative fluorescence-activated cell sorter plots (A) from two pooled independent experiments ($n = 5$ to 10 mice per group). ****, $P \leq 0.0001$; ***, $P \leq 0.001$; *, $P \leq 0.05$. (B, C) Analysis of variance with Tukey's posttest for significance.

these data indicate that i.t. BCG vaccination induced airway-resident T cells with a heightened ability to migrate to the lung and produce the key protective proinflammatory cytokine IFN-γ. Although $CD4^+$ T cells could be categorized as $T_{EM}$ and $T_{RM}$ on the basis of surface markers, transcriptional profiling revealed more heterogeneous populations.

**Mucosal transfer of airway-resident T cell populations confers protection against TB.** To determine the subset(s) of airway-infiltrating T cells critical for improved protection after mucosal vaccination, we adoptively transferred sorted airway T cell subpopulations directly into the tracheas of naive C57BL/6 (B6) mice 1 day prior to an aerogenic *M. tuberculosis* challenge (Fig. 6A; see Fig. S4 in the supplemental material). All of the transferred subsets provided some degree of protection 28 days after the *M. tuberculosis* challenge (Fig. 6B). Intriguingly, transfer of as few as 3,500 sorted $CD8^+$ $T_{RM}$ cells into naive mice conferred the most profound protection against a *M. tuberculosis* challenge, on a per-cell basis (Fig. 6B). Transfer of $CD8^+$ $T_{RM}$ cells was associated with significantly lower AM numbers, higher numbers of $CD4^+$ T cells, and increased numbers of B cells in the lung 28 days after the *M. tuberculosis* challenge (Fig. 6C). We also performed airway $CD4^+$ and $CD8^+$ T cell depletion (Fig. S5; see Fig. S6). These experiments yielded an opposite effect compared to the transfer of different T cell subsets (Fig. 6C). Whereas the mucosal $CD4^+$ T

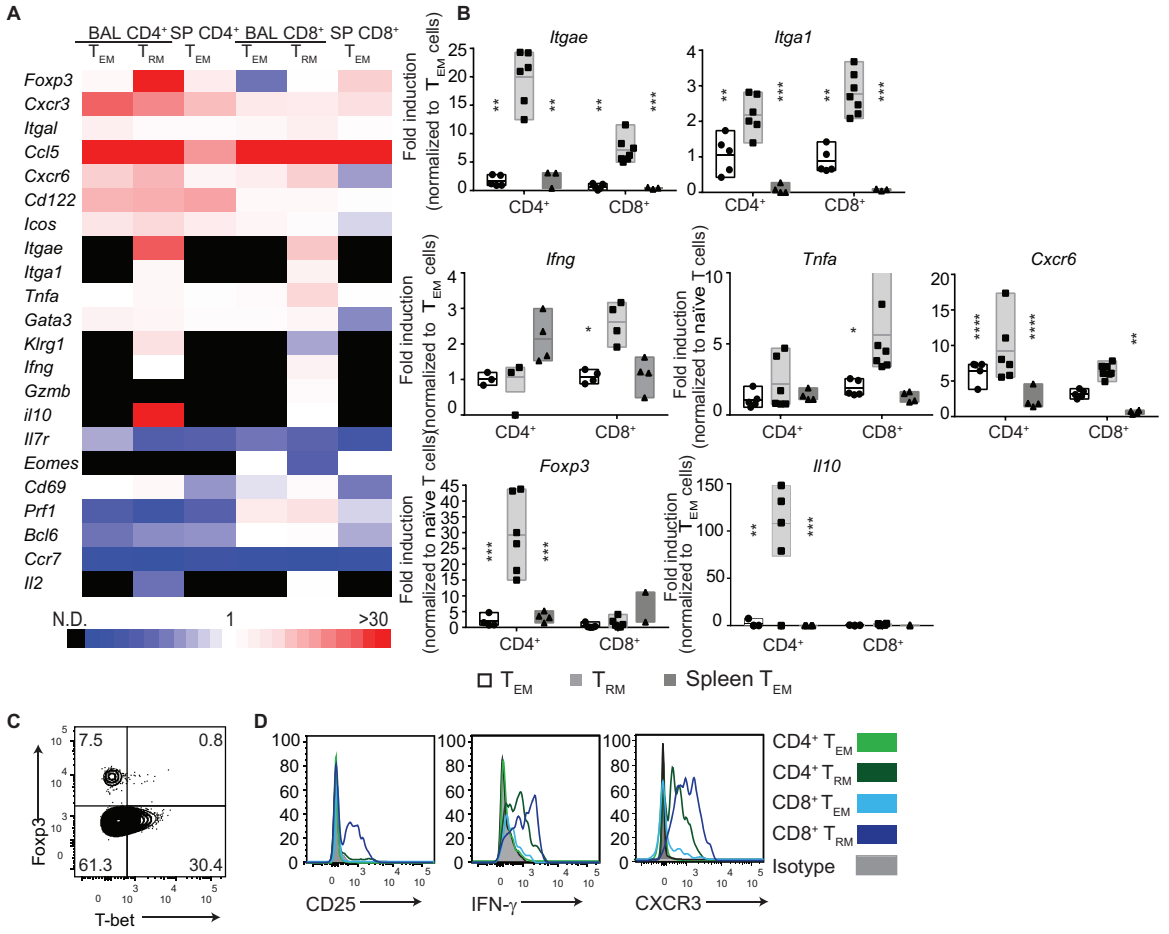


**FIG 5** Phenotypic characterization of lung-infiltrating T cells generated by i.t. BCG vaccination (A, B). B6 mice were BCG vaccinated i.t., and BALF T cell subsets were sorted 60 days later by fluorescence-activated cell sorting gated as described in the legend to Fig. 4A. Sorted naive (TCR$\beta^+$ CD44$^{lo}$ CD62L$^{hi}$) BALF T cells or splenic $T_{EM}$ cells (TCR$\beta^+$ CD44$^{hi}$ CD62L$^{lo}$) from i.t. BCG-vaccinated mice 60 days after immunization were also used as controls. (A) Heat map showing gene expression from sorted BALF T cell populations. Triplicates of 100 BALF CD4$^+$ and CD8$^+$ $T_{EM}$ and $T_{RM}$ cells from i.t. BCG-vaccinated mice were sorted. Quantitative PCR was run with the data collection software (36 cycles) from Fluidigm. mRNA concentrations of all sorted T cell populations were normalized to $\beta$-actin (NM_007393.4) expression. The color code indicates fold changes ($2^{-\Delta\Delta CT}$) in transcripts relative to the appropriate internal control as indicated. (B) Fold changes in the expression of selected genes of sorted BALF CD4$^+$ and CD8$^+$ $T_{EM}$ and $T_{RM}$ cells from i.t. BCG-vaccinated mice compared to the appropriate internal control. Quantitative PCR was run with the data collection software (36 cycles) from Fluidigm as described for panel A. (C, D) BALF immune cell phenotype measured by flow cytometry 60 days after i.t. BCG vaccination. (C) Representative flow cytometry of intracellular Foxp3 and T-bet expression by sorted CD4$^+$ $T_{RM}$ cells. (D) Representative histograms of selected surface activation markers and IFN-$\gamma$ expression by CD4$^+$ and CD8$^+$ $T_{EM}$ and $T_{RM}$ cells. Results are presented as pooled individual data points ± the standard error of the mean (B), representative fluorescence-activated cell sorter plots (C), or histograms (D) from two pooled independent experiments ($n = 6$ to 8 mice per group). The statistical significance of differences from the $T_{RM}$ cell subset (B) is shown. ****, $P \leq 0.0001$; ***, $P \leq 0.001$; **, $P \leq 0.01$; *, $P \leq 0.05$. (B) Analysis of variance with Tukey's posttest for significance.

cell depletion efficiency was around 90%, the CD8$^+$ T cell depletion efficiency was only around 50% (data not shown). Because of the low efficiency of CD8$^+$ T cell depletion, we could not draw any definitive conclusions. Therefore, despite its great additive value to the overall conclusion, we were not able to specifically delete $T_{RM}$ cell populations from the airway.

Intriguingly, when the bacterial load in the whole lung was determined without previously performing lavage, the transfer of all airway T cell subsets reduced bacterial loads at equal levels and the improved protective effect of CD8$^+$ $T_{RM}$ cells was lost (Fig. 6D). These results suggest that i.t. BCG vaccination induces (i) multiple subpopulations of local $T_{RM}$ cells that contribute to protection against *M. tuberculosis* and (ii) compartmentalized protective effects in lung airways but not in lung parenchyma.

**Oral and i.n. vaccinations mimic i.t. BCG vaccination.** Finally, although the i.t. BCG administration employed in our model is a low-invasion intervention, it is unlikely to be broadly applicable as a human vaccination strategy. Clinically more feasible intranasal (i.n.) and oral BCG vaccinations strikingly induced infiltration of T cells into the lung parenchyma and airways very similar to that induced by i.t. BCG vaccination, which was reflected in overall increased numbers of $T_{EM}$ and $T_{RM}$ cells (Fig. 7A), as well as *Mycobacterium*-specific T cells expressing CXCR3 (Fig. 7B and C; see Fig. S7). Together with published observations regarding improved *M. tuberculosis* control following i.n. and oral BCG vaccinations (30, 31), our data indicate that mucosal BCG vaccination promotes protection via potent induction of lung parenchyma- and airway-resident memory CD4$^+$ and

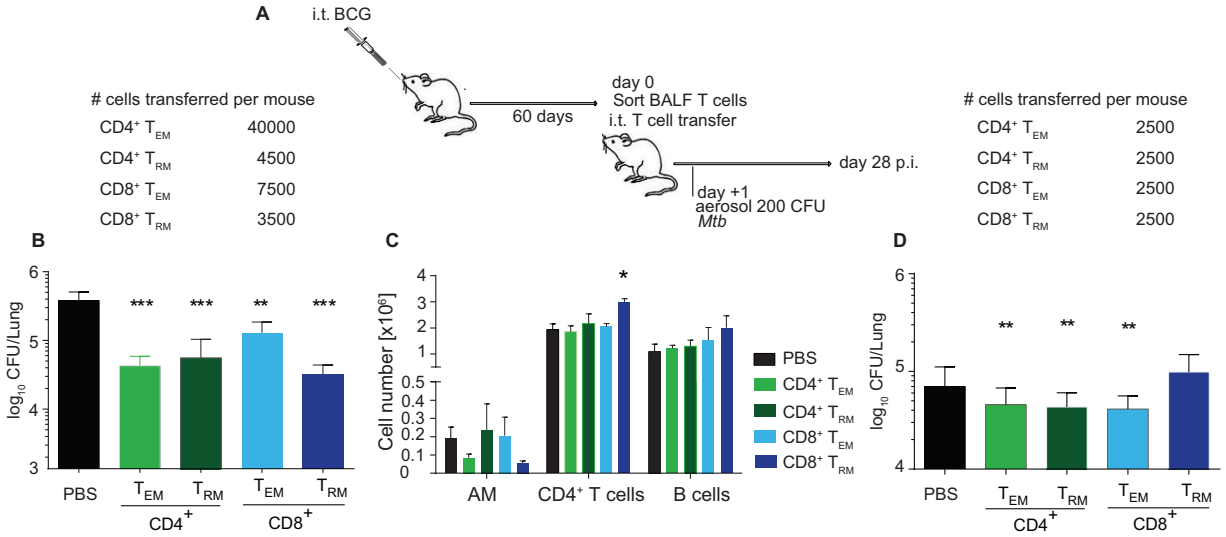


**FIG 6** Mucosal transfer of airway-resident T cell populations confers protection against TB. (A) B6 mice were BCG vaccinated i.t., and BALF T cell subsets were sorted 60 days later by fluorescence-activated cell sorting. BALF $CD4^+$ and $CD8^+$ $T_{EM}$ and $T_{RM}$ cells were sorted as depicted in Fig. 4A. The sorted T cell population purity was assessed as >86%. From $0.25 \times 10^4$ to $4 \times 10^4$ sorted cells were i.t. transferred into naive B6 mice (B, D). The numbers of cells transferred are indicated at the top. The following day, recipient mice were aerosol infected with *M. tuberculosis* and lung CFU counts were determined 28 days later. (B, D) Bacterial CFU counts in lung tissue after BALF removal (B) and in airways and tissue without lavage (D). (C) Immune cellular composition in the lung parenchyma 28 days p.i following i.t. transfer of sorted BALF T cell populations from i.t. BCG-vaccinated mice. Cell numbers are representative of one of two experiments performed as described for panel B. The statistical significance of differences from the i.t. PBS control is shown. Results are presented as mean pooled data ± the standard error of the mean (B to D) from one representative (B, C) or two pooled independent experiments (D) ($n = 3$ mice per group [B, C] or $n = 6$ to 8 mice per group [D]). ****, $P \leq 0.0001$; ***, $P \leq 0.001$; **, $P \leq 0.01$; *, $P \leq 0.05$. (B to D) Analysis of variance with Tukey's posttest for significance.

$CD8^+$ T cells, comprising mixed $CD4^+$ T cell populations and $CD8^+$ $T_{RM}$ cells.

## DISCUSSION

We describe an in-depth *in vivo* approach to dissection of the immunological mechanisms associated with improved protection of mucosal BCG vaccination against pulmonary TB. We conclude that lung-resident $CD4^+$ and $CD8^+$ T cells, comprising $CD8^+$ $T_{RM}$ cells, are a main component underlying the enhanced efficacy of mucosal BCG administration. Airway-resident $CD4^+$ T cells comprised a mixture of T-bet$^+$ effector and Foxp3$^+$-expressing regulatory T cells. In contrast, airway-resident $CD8^+$ T cells displayed prototypical $T_{RM}$ features and expressed IFN-$\gamma$ and TNF-$\alpha$, two major mediators of protective immunity against *M. tuberculosis*.

It has been previously shown that transfer of total lung T cells following i.n. but not s.c. vaccination with *M. tuberculosis* culture filtrate proteins can protect against TB (15). Aerosol administration of an attenuated *M. tuberculosis* vaccine candidate, *M. tuberculosis* Δ*sigH*, has also been reported to be highly effective in preventing TB in nonhuman primates via induction of local T cell responses (19). These findings validate the superiority of mucosal vaccination in generating a robust and effective T cell response against *M. tuberculosis*. As the most striking effect of i.t. BCG vaccination we identified a prominent subpopulation of $CD8^+$ $T_{RM}$ cells in the lung airways bearing the prototypic $CD69^+$ $CD103^+$ surface phenotype associated with tissue sequestration (32, 33). Many coexpressed the mucosal and lung-homing markers CD103 (*Itgae*) and VLA-1 (*Itga1*). CD69, an early leukocyte activation marker, can interact with S1P1 and downregulate its expression, leading to prolonged T cell retention and local memory formation (34). CD103 on T cells binds to epithelial E-cadherin in diverse organs such as the skin and gut (27). Our finding that CD103 is surface expressed, especially by $CD8^+$ $T_{RM}$ cells in the lung following mycobacterial lung infection, extends its relevance to lung-residing memory T cell responses. VLA-1, $\alpha 1\beta 1$-integrin, is an adhesion molecule known to be highly expressed by respiratory virus-specific memory $CD8^+$ T cells in the airways, retaining them in the lung through attachment to the extracellular matrix (35). Our study is the first to ascribe protective relevance to intraluminal T cells following mucosal BCG vaccination, which includes $CD8^+$ $T_{RM}$ cells in the lung airways in the context of TB.

$CD8^+$ $T_{RM}$ cells have been implicated in protection following viral infections (36), but their beneficial role following bacterial infection is just being appreciated (37). Recent work has highlighted the potential of $CD8^+$ $T_{RM}$ to activate bystander NK and B cells via IFN-$\gamma$, TNF-$\alpha$, and IL-2, in addition to their well-known cytolytic role (24). Mucosal i.t. transfer of airway T cell populations into naive mice identified a crucial role for $CD8^+$ $T_{RM}$ cells in conferring lung protection in our study. Intriguingly, when BALF was collected from infected mice prior to CFU enumeration, transferred $CD8^+$ $T_{RM}$ not only displayed superior protection against an *M. tuberculosis* challenge but also reduced the number of AMs and increased the local $CD4^+$ T and B cell numbers. In contrast, when CFU counts in the complete lung (BALF plus lung tissue) were determined, the protective capacity of transferred $CD8^+$ $T_{RM}$ cells was lower. Thus, it is tempting to speculate that cytolytic $CD8^+$ $T_{RM}$ cells limit the entry of *M. tuberculosis* into lung tissue by killing infected AMs in the lung airways, constraining the cellular reservoir for *M. tuberculosis*. It is also possible that $CD8^+$ $T_{RM}$ cells contribute to protective immunity attained by i.t. BCG vaccination in the lung (i) by means of killing infected AMs and (ii) by recruiting $CD4^+$ T cells to the site

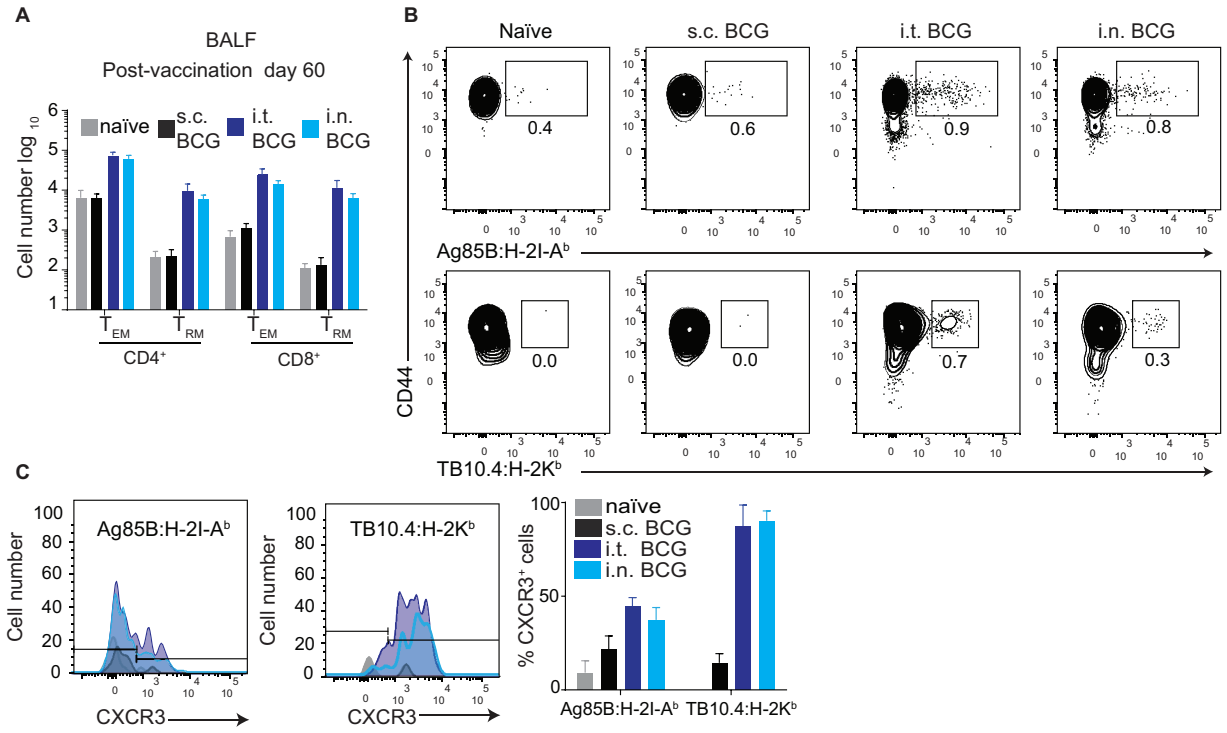


**FIG 7** I.n. BCG vaccination mimics i.t. BCG vaccination. (A to C) BALF characterization at day 60 after BCG vaccination. (A) Quantification of BALF TCR$\beta^+$ CD4$^+$ and CD8$^+$ T cell and $T_{EM}$ and $T_{RM}$ cell numbers by flow cytometry. (B) Flow cytometry gating strategy for Ag85B:H-2I-A$^b$ CD4$^+$ and TB10.4:H-2K$^b$ CD8$^+$ T cells pregated on TCR$\beta^+$ CD4$^+$ or CD8$^+$ T cells. (C) Representative histogram showing CXCR3 expression by Ag85B:H-2I-A$^b$ CD4$^+$ and TB10.4:H-2K$^b$ CD8$^+$ T cells (left) and their percentage of expression by Ag85B:H-2I-A$^b$ CD4$^+$ and TB10.4:H-2K$^b$ CD8$^+$ T cells following BCG vaccination (49). Results are presented as pooled mean data ± the standard error of the mean (A, C), as representative fluorescence-activated cell sorter plots (B), or as histograms (C) from two pooled independent experiments ($n = 8$).

of *M. tuberculosis* infection. CD8$^+$ $T_{RM}$ cells' killing abilities, as well as their compartmentalized protective role, should be addressed in future studies.

Comprehensive transcriptional and flow cytometric analysis of airway CD4$^+$ memory T cells identified a heterogeneous population comprising Foxp3$^+$- or T-bet$^+$-expressing T cell subsets. Further studies are needed to analyze the functional properties of CD103$^-$ CD69$^+$ CD4$^+$ memory T cells that have been described by others as most concordant to the CD4$^+$ $T_{RM}$ population (38). In addition, enhanced IL-10 transcripts suggest diverse roles for lung CD4$^+$ T cells besides the classical Th1 responses previously considered correlates of protection. Although it was beyond the scope of this study to dissect the underlying protective mechanism, CD4$^+$ Foxp3$^+$ T-cell-derived IL-10 emerges as a strong candidate for ameliorating immunopathology (39) and at the same time has been shown to promote the maturation of CD8$^+$ T cells (40). The exact role of airway-resident CD4$^+$ T-cell-derived IL-10 and its functional impact on local anti-*M. tuberculosis* immunity should be elucidated in future studies.

Further studies are required to dissect the mechanisms of protection induced by the transfer of total BALF. A minute number of influenza virus-specific CD8$^+$ T cells in the airways was recently shown to be sufficient to transfer protection against a subsequent influenza virus infection (36). Therefore, it is possible that even fewer than the 2,500 lung-resident T cells induced by BCG vaccination that were transferred here could mediate protection after mucosal transfer. Although it is beyond the scope of this study, identifying the minimal number of T cells required to transfer protection will be valuable additional information.

Some remaining questions need to be addressed in future studies to determine the role of live antigen in the lung following mucosal BCG vaccination. Although the cellular analyses of the lung revealed similar results with s.c. and i.t. BCG-vaccinated mice, the presence of a low-grade ongoing infection in the lungs hampers the use of CD44 as a memory marker, as CD44 is also a marker of effector cells during ongoing infection. The crossover of CD69 as both an early activation marker and a resident memory marker requires further transfer experiments with T cell subpopulations to address their long-term viability and recall responses in the absence of antigen in order to validate them as "true" memory populations. Because there are no singular defining markers for $T_{RM}$ cells yet, particularly for the CD4$^+$ subset, in this study, we chose to perform mRNA phenotyping of CD4 and CD8 T cells infiltrating the airways postvaccination, which revealed heterogeneous expression of transcription factors and effector molecules and confirmed their ability to mount a recall response to an infectious challenge. Furthermore, it will also be important to determine the contribution of non-*M. tuberculosis*-specific memory T cells (e.g., influenza virus-specific T cells) in mediating protection after adoptive transfer. Although unspecific mechanisms for protection cannot be ruled out entirely, the fact that not all *M. tuberculosis*-specific T cell subsets protected equally well after adoptive transfer suggests that non-*M. tuberculosis*-specific effects (41) contribute little to protection against TB following vaccination.

Nevertheless, only transfer of *M. tuberculosis*-unrelated memory T cell subsets from the lung will definitively address the role of noncognate effects.

Taken together, our results highlight the value of better understanding the mechanisms underlying mucosal vaccination against TB. Our findings emphasize that mucosal vaccination offers an option for improving protective efficacy against TB either by BCG or by second-generation vaccine candidates. We recommend that optimization of mucosal vaccine administration should complement the design of novel vaccine candidates that either substitute for or boost BCG immunization.

## MATERIALS AND METHODS

**Animals and bacteria.** B6 mice were maintained under specific-pathogen-free conditions. All experiments were conducted in accordance with the requirements of and approval by the State Office for Health and Social Services. *M. tuberculosis* strain H37Rv (ATCC no. 27294) and BCG SSI 1331 (ATCC no. 35733) were grown by previously described protocols (42). Prior to vaccination, vaccine stock vials were thawed and cells were harvested and resuspended in phosphate-buffered saline (PBS). For CFU enumeration, serial dilutions were performed and plated onto Middlebrook 7H11 agar. Plates were incubated at 37°C for 3 to 4 weeks prior to counting.

**Immunizations and infection.** B6 mice were immunized with $5 \times 10^5$ (i.t. and i.n.), $1 \times 10^6$ (s.c.), or $1 \times 10^8$ (oral) CFU (12, 31, 43). For i.t. immunization, anesthetized mice (1:1:8 xylazine-ketamine-PBS) were inoculated in the oropharynx with 50 $\mu$l of bacteria (44). To determine protective efficacy, mice were challenged via the aerosol route with 200 CFU of *M. tuberculosis* H37Rv 60 days postvaccination by using a Glas-Col inhalation exposure system.

**Histology and IF assay.** Unperfused lungs from BCG-vaccinated or *M. tuberculosis*-infected animals were fixed for 24 h in 4% (wt/vol) paraformaldehyde and then dehydrated and embedded in paraffin for histological analysis. Two-micrometer sections were deparaffinized and stained with hematoxylin and eosin (H&E). For immunofluorescence (IF) assay, heat-induced antigen retrieval in citrate buffer (10 mM citric acid, 0.05% Tween 20, pH 6.0) was performed prior to incubation with anti-CD31 (clone SZ31; Dianova), anti-CD3 (clone M-20; Santa Cruz), and anti-CD4 (clone 4SM95; eBioscience) antibodies.

**Cell isolation.** Intra-airway luminal cells were removed from the lung by bronchial lavage as described previously (45). Supernatant was frozen at −80°C until protein analysis, and the remaining cells were analyzed by flow cytometry. Lungs were perfused with PBS through the left ventricle and cut into small pieces, and single-cell suspensions were prepared by mechanical dissociation through a 70-$\mu$m nylon mesh (46).

**Flow cytometry, intracellular cytokine staining, and tetramer staining.** Identification of innate cell populations was performed with antibodies against CD11b (M1/70), CD11c (HL3), Ly6G (1A8), Siglec-F (E50-2440), F4/80 (BM8), and MHC class II (M5/114.15.2). Surface identification of T cells was performed with antibodies against T cell receptor $\beta$ (TCR$\beta$) (H57-597), CD4 (GK1.5), CD8 (53-6.7), CD44 (IM7), CD62L (MEL-14), CD103 (M290), and CD69 (H1.2F3). For memory phenotyping, CXCR3 (CXCR3-173) and CD25 (PC61.5) antibodies were included. DCs were characterized as CD11c$^{hi}$ MHC-II$^{hi}$, AMs were characterized as CD11c$^{hi}$ Siglec-F$^{hi}$ CD11b$^{low\text{-}int}$ autofluorescence positive, neutrophils were characterized as Ly6G$^{hi}$ CD11b$^{hi}$, eosinophils were characterized as CD11c$^{low/-}$ Siglec-F$^{hi}$, NK cells were characterized as TCR$\beta$-NK1.1$^+$, and CD4$^+$ and CD8$^+$ T cells were characterized as TCR$\beta^+$ CD4$^+$ or TCR$\beta^+$ CD8$^+$. Intracellular staining for transcription factors Foxp3 (FJK-16s) and T-bet (4B10) was performed with the Foxp3 staining buffer kit (eBioscience). To determine IFN-$\gamma$ (4S.B3) cytokine levels, intracellular staining was performed with the BD Cytofix/Cytoperm Fixation/permeabilization kit according to manufacturer's instructions.

Ag85B:H-2I-A$^b$ (280 to 294: FQDAYNAAGGHNAVF) tetramers were provided by the National Institutes of Health tetramer facility, and TB10.4:H-2K$^b$ (4 to 11: IMYNYPAM) tetramers were prepared in house. Tetramer staining was performed at room temperature for 1 h prior to additional surface staining. Analysis was performed on an LSR II or Canto II (Becton, Dickinson) flow cytometer. Data were analyzed with FlowJo (TreeStar).

**Mucosal T cell transfer.** CD4$^+$ and CD8$^+$ $T_{EM}$ and $T_{RM}$ cells were sorted from BALF collected from i.t. BCG-vaccinated mice 60 days postvaccination. B6 recipient mice were anesthetized and received 50 $\mu$l of a cell suspension in PBS containing sorted T cell populations i.t. The specific cell numbers transferred are indicated in the figures.

**Mucosal T cell depletion.** B6 mice were BCG vaccinated i.t., and 2 days prior to a challenge, CD4 and CD8 T cell subsets were mucosally depleted through i.t. administration of anti-CD4 (GK1.5), anti-CD8 (53-6.7), or anti-control IgG (Ctrl). Two days following mucosal depletion, depleted and untreated mice were aerosol infected with *M. tuberculosis* and lung CFU counts were determined 28 days later.

**Gene expression analysis.** Gene expression was analyzed simultaneously with the 48.48 Dynamic Array Integrated Fluidic Circuits from Fluidigm as previously described (47). Preamplification of genes by reverse transcription and cDNA synthesis (18 cycles) was performed with the Cells Direct one-Step qPCR kit (Life Technologies, Inc.) and TaqMan gene expression assay mix (Applied Biosystems). Triplicates of 100 BALF or lung parenchyma cells were sorted, and mRNA amounts were normalized to $\beta$-actin (NM_007393.4) expression. Data represent fold changes ($2^{-\Delta\Delta CT}$) in transcripts relative to the appropriate internal control.

**Statistical analyses.** Statistical analyses were performed with GraphPad Prism software (San Diego, CA). For *in vivo* experiments, data from two independent experiments were pooled. $P$ values of $<0.05$ were considered statistically significant.

## SUPPLEMENTAL MATERIAL

Supplemental material for this article may be found at http://mbio.asm.org/lookup/suppl/doi:10.1128/mBio.01686-16/-/DCSupplemental.

Figure S1, EPS file, 1 MB.
Figure S2, EPS file, 3.1 MB.
Figure S3, EPS file, 1 MB.
Figure S4, EPS file, 1.3 MB.
Figure S5, EPS file, 0.9 MB.
Figure S6, EPS file, 1.1 MB.
Figure S7, EPS file, 0.6 MB.

## ACKNOWLEDGMENTS

C.P. was supported by the International Max Planck Research School (IMPRS-IDI), S.H.E.K. was supported by the Max Planck Society and the European Union's Seventh Framework Programme (EU FP7) project ADITEC (HEALTH-F4-2011-280873), A.K. was supported by the National Health and Medical Research Council of Australia through a CJ Martin Biomedical Early Career Fellowship (APP1052764).

We thank M. L. Grossman for editorial assistance and A. Dorhoi for critically reading the manuscript. We also thank the reviewers for their constructive comments, some of which have been included in this paper.

## REFERENCES

1. **Calmette A.** 1927. La vaccination préventive contre la tuberculose par le 'BCG'. Masson & Co., Paris, France.
2. **Trunz BB, Fine P, Dye C.** 2006. Effect of BCG vaccination on childhood tuberculous meningitis and miliary tuberculosis worldwide: a meta-analysis and assessment of cost-effectiveness. Lancet **367:**1173–1180. http://dx.doi.org/10.1016/S0140-6736(06)68507-3.
3. **WHO.** 2015, Global tuberculosis report. World Health Organization, Geneva, Switzerland.
4. **Kaufmann SH.** 2013. Tuberculosis vaccines: time to think about the next generation. Semin Immunol **25:**172–181. http://dx.doi.org/10.1016/j.smim.2013.04.006.
5. **StopTB Partnership.** 2014. StopTB Partnership 2014 annual report. United Nations Office for Project Services, U.N. City, Copenhagen, Den-

mark. http://www.stoptb.org/assets/documents/resources/publications/annualreports/STOPTB_annualeport_2014_web.pdf.
6. **Ottenhoff TH, Kaufmann SH.** 2012. Vaccines against tuberculosis: where are we and where do we need to go? PLoS Pathog **8:**e1002607. http://dx.doi.org/10.1371/journal.ppat.1002607.
7. **Cowley SC, Elkins KL.** 2003. CD4$^+$ T cells mediate IFN-gamma-independent control of *Mycobacterium tuberculosis* infection both in vitro and in vivo. J Immunol **171:**4689–4699. http://dx.doi.org/10.4049/jimmunol.171.9.4689.
8. **Andersen P, Smedegaard B.** 2000. CD4(+) T-cell subsets that mediate immunological memory to *Mycobacterium tuberculosis* infection in mice. Infect Immun **68:**621–629. http://dx.doi.org/10.1128/IAI.68.2.621-629.2000.
9. **Beverley PC, Sridhar S, Lalvani A, Tchilian EZ.** 2014. Harnessing local and systemic immunity for vaccines against tuberculosis. Mucosal Immunol **7:**20–26. http://dx.doi.org/10.1038/mi.2013.99.
10. **Monteiro-Maia R, de Pinho RT.** 2014. Oral bacillus Calmette-Guerin vaccine against tuberculosis: why not? Mem Inst Oswaldo Cruz **109:**838–845. http://dx.doi.org/10.1590/0074-0276140091.
11. **Manjaly Thomas ZR, McShane H.** 2015. Aerosol immunisation for TB: matching route of vaccination to route of infection. Trans R Soc Trop Med Hyg **109:**175–181. http://dx.doi.org/10.1093/trstmh/tru206.
12. **Aguilo N, Toledo AM, Lopez-Roman EM, Perez-Herran E, Gormley E, Rullas-Trincado J, Angulo-Barturen I, Martin C.** 2014. Pulmonary *Mycobacterium bovis* BCG vaccination confers dose-dependent superior protection compared to that of subcutaneous vaccination. Clin Vaccine Immunol **21:**594–597. http://dx.doi.org/10.1128/CVI.00700-13.
13. **Chen X, Xiu F, Horvath CN, Damjanovic D, Thanthrige-Don N, Jeyanathan M, Xing Z.** 2012. Regulation of TB vaccine-induced airway luminal T cells by respiratory exposure to endotoxin. PLoS One **7:**e41666. http://dx.doi.org/10.1371/journal.pone.0041666.
14. **Teijaro JR, Turner D, Pham Q, Wherry EJ, Lefrançois L, Farber DL.** 2011. Cutting edge: tissue-retentive lung memory CD4 T cells mediate optimal protection to respiratory virus infection. J Immunol **187:**5510–5514. http://dx.doi.org/10.4049/jimmunol.1102243.
15. **Horvath CN, Shaler CR, Jeyanathan M, Zganiacz A, Xing Z.** 2012. Mechanisms of delayed anti-tuberculosis protection in the lung of parenteral BCG-vaccinated hosts: a critical role of airway luminal T cells. Mucosal Immunol **5:**420–431. http://dx.doi.org/10.1038/mi.2012.19.
16. **Unsoeld H, Pircher H.** 2005. Complex memory T-cell phenotypes revealed by coexpression of CD62L and CCR7. J Virol **79:**4510–4513. http://dx.doi.org/10.1128/JVI.79.7.4510-4513.2005.
17. **Sallusto F, Lenig D, Förster R, Lipp M, Lanzavecchia A.** 1999. Two subsets of memory T lymphocytes with distinct homing potentials and effector functions. Nature **401:**708–712. http://dx.doi.org/10.1038/44385.
18. **Gebhardt T, Wakim LM, Eidsmo L, Reading PC, Heath WR, Carbone FR.** 2009. Memory T cells in nonlymphoid tissue that provide enhanced local immunity during infection with herpes simplex virus. Nat Immunol **10:**524–530. http://dx.doi.org/10.1038/ni.1718.
19. **Kaushal D, Foreman TW, Gautam US, Alvarez X, Adekambi T, Rangel-Moreno J, Golden NA, Johnson AM, Phillips BL, Ahsan MH, Russell-Lodrigue KE, Doyle LA, Roy CJ, Didier PJ, Blanchard JL, Rengarajan J, Lackner AA, Khader SA, Mehra S.** 2015. Mucosal vaccination with attenuated *Mycobacterium tuberculosis* induces strong central memory responses and protects against tuberculosis. Nat Commun **6:**8533. http://dx.doi.org/10.1038/ncomms9533.
20. **Aguilo N, Alvarez-Arguedas S, Uranga S, Marinova D, Monzón M, Badiola J, Martin C.** 2016. Pulmonary but not subcutaneous delivery of BCG vaccine confers protection to tuberculosis-susceptible mice by an interleukin 17-dependent mechanism. J Infect Dis **213:**831–839. http://dx.doi.org/10.1093/infdis/jiv503.
21. **Lalvani A.** 2004. Counting antigen-specific T cells: a new approach for monitoring response to tuberculosis treatment? Clin Infect Dis **38:**757–759. http://dx.doi.org/10.1086/381763.
22. **Kohlmeier JE, Cookenham T, Miller SC, Roberts AD, Christensen JP, Thomsen AR, Woodland DL.** 2009. CXCR3 directs antigen-specific effector CD4$^+$ T cell migration to the lung during parainfluenza virus infection. J Immunol **183:**4378–4384. http://dx.doi.org/10.4049/jimmunol.0902022.
23. **Wu T, Hu Y, Lee YT, Bouchard KR, Benechet A, Khanna K, Cauley LS.** 2014. Lung-resident memory CD8 T cells (TRM) are indispensable for optimal cross-protection against pulmonary virus infection. J Leukoc Biol **95:**215–224. http://dx.doi.org/10.1189/jlb.0313180.
24. **Schenkel JM, Fraser KA, Beura LK, Pauken KE, Vezys V, Masopust D.** 2014. T cell memory. Resident memory CD8 T cells trigger protective innate and adaptive immune responses. Science **346:**98–101. http://dx.doi.org/10.1126/science.1254536.
25. **Gebhardt T, Mueller SN, Heath WR, Carbone FR.** 2013. Peripheral tissue surveillance and residency by memory T cells. Trends Immunol **34:**27–32. http://dx.doi.org/10.1016/j.it.2012.08.008.
26. **Cauley LS, Lefrançois L.** 2013. Guarding the perimeter: protection of the mucosa by tissue-resident memory T cells. Mucosal Immunol **6:**14–23. http://dx.doi.org/10.1038/mi.2012.96.
27. **Mackay LK, Rahimpour A, Ma JZ, Collins N, Stock AT, Hafon ML, Vega-Ramos J, Lauzurica P, Mueller SN, Stefanovic T, Tscharke DC, Heath WR, Inouye M, Carbone FR, Gebhardt T.** 2013. The developmental pathway for CD103(+)CD8$^+$ tissue-resident memory T cells of skin. Nat Immunol **14:**1294–1301. http://dx.doi.org/10.1038/ni.2744.
28. **Koch MA, Tucker-Heard G, Perdue NR, Killebrew JR, Urdahl KB, Campbell DJ.** 2009. The transcription factor T-bet controls regulatory T cell homeostasis and function during type 1 inflammation. Nat Immunol **10:**595–602. http://dx.doi.org/10.1038/ni.1731.
29. **Lee LN, Ronan EO, de Lara C, Franken KL, Ottenhoff TH, Tchilian EZ, Beverley PC.** 2011. CXCR6 is a marker for protective antigen-specific cells in the lungs after intranasal immunization against *Mycobacterium tuberculosis*. Infect Immun **79:**3328–3337. http://dx.doi.org/10.1128/IAI.01133-10.
30. **Giri PK, Sable SB, Verma I, Khuller GK.** 2005. Comparative evaluation of intranasal and subcutaneous route of immunization for development of mucosal vaccine against experimental tuberculosis. FEMS Immunol Med Microbiol **45:**87–93. http://dx.doi.org/10.1016/j.femsim.2005.02.009.
31. **Hosseini M, Dobakhti F, Pakzad SR, Ajdary S.** 2015. Immunization with single oral dose of alginate-encapsulated BCG elicits effective and long-lasting mucosal immune responses. Scand J Immunol **82:**489–497. http://dx.doi.org/10.1111/sji.12351.
32. **Hogan RJ, Zhong W, Usherwood EJ, Cookenham T, Roberts AD, Woodland DL.** 2001. Protection from respiratory virus infections can be mediated by antigen-specific CD4(+) T cells that persist in the lungs. J Exp Med **193:**981–986. http://dx.doi.org/10.1084/jem.193.8.981.
33. **Turner DL, Farber DL.** 2014. Mucosal resident memory CD4 T cells in protection and immunopathology. Front Immunol **5:**331. http://dx.doi.org/10.3389/fimmu.2014.00331.
34. **Mackay LK, Braun A, Macleod BL, Collins N, Tebartz C, Bedoui S, Carbone FR, Gebhardt T.** 2015. Cutting edge: CD69 interference with sphingosine-1-phosphate receptor function regulates peripheral T cell retention. J Immunol **194:**2059–2063. http://dx.doi.org/10.4049/jimmunol.1402256.
35. **Ray SJ, Franki SN, Pierce RH, Dimitrova S, Koteliansky V, Sprague AG, Doherty PC, de Fougerolles AR, Topham DJ.** 2004. The collagen binding alpha1beta1 integrin VLA-1 regulates CD8 T cell-mediated immune protection against heterologous influenza infection. Immunity **20:**167–179. http://dx.doi.org/10.1016/S1074-7613(04)00021-4.
36. **Slütter B, Pewe LL, Kaech SM, Harty JT.** 2013. Lung airway-surveilling CXCR3(hi) memory CD8(+) T cells are critical for protection against influenza A virus. Immunity **39:**939–948. http://dx.doi.org/10.1016/j.immuni.2013.09.013.
37. **Stary G, Olive A, Radovic-Moreno AF, Gondek D, Alvarez D, Basto PA, Perro M, Vrbanac VD, Tager AM, Shi J, Yethon JA, Farokhzad OC, Langer R, Starnbach MN, von Andrian UH.** 2015. Vaccines. A mucosal vaccine against *Chlamydia trachomatis* generates two waves of protective memory T cells. Science **348:**aaa8205. http://dx.doi.org/10.1126/science.aaa8205.
38. **Mueller SN, Mackay LK.** 2016. Tissue-resident memory T cells: local specialists in immune defence. Nat Rev Immunol **16:**79–89. http://dx.doi.org/10.1038/nri.2015.3.
39. **Couper KN, Blount DG, Riley EM.** 2008. IL-10: the master regulator of immunity to infection. J Immunol **180:**5771–5777. http://dx.doi.org/10.4049/jimmunol.180.9.5771.
40. **Laidlaw BJ, Cui W, Amezquita RA, Gray SM, Guan T, Lu Y, Kobayashi Y, Flavell RA, Kleinstein SH, Craft J, Kaech SM.** 2015. Production of IL-10 by CD4(+) regulatory T cells during the resolution of infection promotes the maturation of memory CD8(+) T cells. Nat Immunol **16:**871–879. http://dx.doi.org/10.1038/ni.3224.
41. **Kupz A, Zedler U, Stäber M, Perdomo C, Dorhoi A, Brosch R, Kaufmann SH.** 2016. ESAT-6-dependent cytosolic pattern recognition drives

noncognate tuberculosis control in vivo. J Clin Invest **126:**2109–2122. http://dx.doi.org/10.1172/JCI84978.

42. **Rao M, Vogelzang A, Kaiser P, Schuerer S, Kaufmann SH, Gengenbacher M.** 2013. The tuberculosis vaccine candidate bacillus Calmette-Guerin DeltaureC::hly coexpressing human interleukin-7 or −18 enhances antigen-specific T cell responses in mice. PLoS One **8:**e78966. http://dx.doi.org/10.1371/journal.pone.0078966.
43. **Derrick SC, Kolibab K, Yang A, Morris SL.** 2014. Intranasal administration of *Mycobacterium bovis* BCG induces superior protection against aerosol infection with *Mycobacterium tuberculosis* in mice. Clin Vaccine Immunol **21:**1443–1451. http://dx.doi.org/10.1128/CVI.00394-14.
44. **Rayamajhi M, Redente EF, Condon TV, Gonzalez-Juarrero M, Riches DWH, Lenz LL.** 2011. Non-surgical intratracheal instillation of mice with analysis of lungs and lung draining lymph nodes by flow cytometry. J Vis Exp. http://dx.doi.org/10.3791/2702:10.3791/2702.
45. **Nouailles G, Dorhoi A, Koch M, Zerrahn J, Weiner J III, Faé KC, Arrey F, Kuhlmann S, Bandermann S, Loewe D, Mollenkopf HJ, Vogelzang A, Meyer-Schwesinger C, Mittrücker HW, McEwen G, Kaufmann SH.** 2014. CXCL5-secreting pulmonary epithelial cells drive destructive neutrophilic inflammation in tuberculosis. J Clin Invest **124:**1268–1282. http://dx.doi.org/10.1172/JCI72030.
46. **Vogelzang A, Perdomo C, Zedler U, Kuhlmann S, Hurwitz R, Gengenbacher M, Kaufmann SH.** 2014. Central memory CD4$^+$ T cells are responsible for the recombinant bacillus Calmette-Guerin DeltaureC::hly vaccine's superior protection against tuberculosis. J Infect Dis **210:**1928–1937. http://dx.doi.org/10.1093/infdis/jiu347.
47. **Lozza L, Farinacci M, Faé K, Bechtle M, Stäber M, Dorhoi A, Bauer M, Ganoza C, Weber S, Kaufmann SH.** 2014. Crosstalk between human DC subsets promotes antibacterial activity and CD8$^+$ T-cell stimulation in response to Bacille Calmette-Guerin. Eur J Immunol **44:**80–92. http://dx.doi.org/10.1002/eji.201343797.
48. **Thome JJ, Bickham KL, Ohmura Y, Kubota M, Matsuoka N, Gordon C, Granot T, Griesemer A, Lerner H, Kato T, Farber DL.** 2016. Early-life compartmentalization of human T cell differentiation and regulatory function in mucosal and lymphoid tissues. Nat Med **22:**72–77. http://dx.doi.org/10.1038/nm.4008.
49. **Kaplan G, Post FA, Moreira AL, Wainwright H, Kreiswirth BN, Tanverdi M, Mathema B, Ramaswamy SV, Walther G, Steyn LM, Barry CE III, Bekker LG.** 2003. *Mycobacterium tuberculosis* growth at the cavity surface: a microenvironment with failed immunity. Infect Immun **71:**7099–7108. http://dx.doi.org/10.1128/IAI.71.12.7099-7108.2003.